Investigation on Rational Analytical Model of Tall Bridge Pier

LI Jian-zhong[1] and LIANG Zhi-yao[2], JIAO Chi-yu[3]

[1] *Professor, Dept. of Bridge Engineering, Tongji University, Shanghai, CHINA*
[2] *Engineer, Suzhou Industrial Park Administrative Committee, Suzhou, CHINA*
[3] *PhD candidate, Dept. of Bridge Engineering, Tongji University, Shanghai, CHINA*
Email: lijianzh@ mail.tongji.edu.cn

ABSTRACT :

Two analytical models for a tall pier and a low pier are developed based on the elastic-plastic beam-column element and the elastic-plastic fiber beam-column element. Structural seismic demands such as the rotation of the plastic hinge, the development of the plastic zone, and the displacement at the top of a pier are investigated. The effect of the division density of the elastic-plastic beam-column element on seismic demand is investigated and compared. The results show that seismic demands of a tall pier are different from those of a lower pier due to the higher vibration modes contribution. For a tall pier, the multiple plastic hinges occur at the middle and the bottom of the pier and develop with the increase of the seismic intensity. Furthermore, different element division densities have a significant effect on the plastic rotation demand if multiple plastic hinges appears.

KEYWORDS: Tall Bridge Pier, analytical model, elastic-plastic fiber beam-column element,

1. INTRODUCTION

The mountainous areas in west China are the high seismic zones. In these areas, a lot of multi-span continuous deck highway bridges were built crossing mountain valley. Because of the rugged topography, height of many bridge piers in these areas exceeded 40m, some of them even reached about 100m. A tall pier is distinctly different from a low one in structural specialty in the axial force ratio, the slenderness ratio and the dynamic characteristics.

The literature review has indicated [Li Jianzhong et al., 2005] that higher vibration modes have remarkable effect on tall pier, but some researches on a tall pier generally make use of current seismic design codes which suit a lower pier to investigated demand and capacity of a tall pier [William, 1999; Michael et al., 2003]. The current theory, basing on the pseudo-static test of a lower pier, assumes that only one plastic hinge occurs at bottom and the plastic deform in specified equivalent plastic zone L_p at the bottom of the column. This theory underestimates or ignores the contribution of higher vibration modes and may result a large error.

2. ANALYTICAL ELEMENTS OF PIER

Two kinds of element, the elastic-plastic beam-column element and the elastic-plastic fibre beam-column element are usually used for modelling the nonlinear behaviour of the bridge pier in seismic analysis.

An elastic-plastic beam-column element is composed of an elastic beam element and two rigid-plastic hinges at the ends of element. Idealized elastic-plastic force–deformation curve can be employed in the rigid-plastic hinges. The yield surface of a typical reinforce concrete column cross-section proposed by Bresler can be described by yield strength P_u, M_{yu} and M_{zu}.

On the other hand, an elastic-plastic fibre beam-column element is more and more noticeable with improvement of computer calculation ability, because of its good precision. The flexibility-based elastic-plastic fibre beam-column element is an elaborate nonlinear element to simulate the nonlinear hysteretic properties of RC bilateral bending frame subject to axial force and is testified by many RC frame tests. [Taucer et al., 1991; Mohd Hisham, 1994].

The cross-sections of elastic-plastic fiber beam-column element are subdivided into concrete and reinforce fibers with perfect bond. The element based on the assumption that plane sections remain plane. The nonlinear property of an elastic-plastic fibre beam-column element is from material nonlinearity. Each fiber has a specified stress-strain relationship, which can be specified to represent unconfined concrete, confined concrete, and longitudinal steel reinforcement. In this study, Mander's model [Mander et al., 1988] for confined concrete and unconfined concrete were used to represent the stress-strain behaviour of concrete.

The analytical models are developed from a regular multi-span continuous deck highway bridges. The 30m and 90m piers represent a low pier and a tall one, respectively. The cross-section for 30m and 90m pier, respectively, is plotted in Fig. 1(d). The pier is modelled as a cantilever beam with a lumped masses at nodes and an equivalent superstructure concentrate mass M at the top of the pier. The basic parameters of the pier are summarized in Table 1, and the natural periods and mass participation coefficients of the pier in uncracked condition are shown in Table 2.

The piers are designed for flexure failure prior to shear failure. In order to realize the effect of different analytical models on the seismic response of the column, the two different analytical models, the elastic-plastic element model and the fiber element model, are developed and analyzed with Open Sees [Silvia et al., 2005].

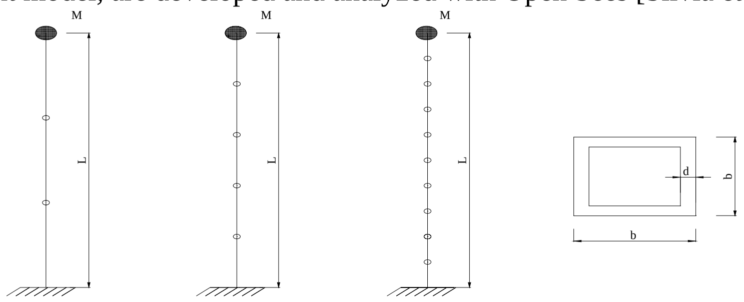

(a) 3 elements (b) 5 elements (c) 10 elements (d) cross-section of pier

Fig. 1 Elastic-plastic element models of pier

Table 1 Basic parameters of piers

Height L/m	Length b/m	Thickness d/m	Superstructure mass M/t	Axial force ratio	Longitudinal steel ratio /%
30	3.2	0.4	700	0.096	1.48
90	4.4	0.5	700	0.130	1.48

Table 2 Natural periods and mass participation coefficients of piers

Height L/m	1st mode		2nd mode		3rd mode	
	Natural period/sec	Mass participation coefficient	Natural period/sec	Mass participation coefficient	Natural period/sec	Mass participation coefficient
30	1.224593	0.8719	0.10291	0.08946	0.039959	0.02596
90	4.093085	0.68547	0.551754	0.17126	0.200671	0.05846

For elastic-plastic element model, to investigate the effects of the element division density on seismic demands, 30m pier model is subdivided into 3, 5, 10, 15, 30 elements, and 90m pier model is subdivided into 3, 10, 20, 30, 45, 90 elements. The yield moment M_y and ultimate moment M_u is obtained from $P-M-\phi$ analysis of corresponding cross-section. In view of reduction of the gross flexural stiffness due to the crack of concrete, effective flexural stiffness, used in elastic-plastic beam-column element model, can be defined in CALTRANS Seismic Design Criteria [CALTRANS, 2001].

$$E_c \times I_{eff} = \frac{M_y}{\phi_y} \tag{2.1}$$

Where, E_c is elastic modulus of concrete,

M_y is moment capacity of the section at first yield of the reinforcing steel,

ϕ_y is yield curvature corresponding to the yield of the first tension reinforcement.

An ensemble of earthquake records (as shown in table 3) are selected for considering the randomness of earthquake ground motions according to different seismic parameters, such as seismic magnitude, Peak Ground Acceleration (PGA) and predominant period. Predominant periods of selected earthquake records vary from 0.1s to 0.92s.

Table 3 Earthquake records

Index	Earthquake Wave	Site	Magnitude	PGA/g	Predominant period/s
E1	1940 El Centro	Imperial Valley	7	0.313	0.46
E2	1995 Kobe	KJMA	6.9	0.821	0.34
E3	1971 San Fernando	Carbon Canyon Dam	6.6	0.071	0.26
E4	1989 Loma Prieta	Alameda Naval Air Stn Hanger	6.9	0.209	0.64
E5	Imperial Valley 1979	Westmorland Fire Station	5.5	0.171	0.1
E6	1999 Turkey	Ambarli	7.1	0.025	0.92
E7	Northridge 1994	Old Ridge Route	6.7	0.514	0.54
E8	Northridge 1994	Las Palmas	6.7	0.357	0.2
E9	Kern County 1952	Taft Lincoln School	7.4	0.178	0.44
E10	Tabas, Iran 1978	Tabas	7.4	0.852	0.2
E11	Hollister 1974	Hollister City Hall	5.2	0.177	0.3
E12	Tangshan 1976	Beijing Hotel	7.8	0.066	0.4

3. SEISMIC DEMAND ANALYSIS OF PIERS

3.1. Low pier

In order to investigate the effect of the element division density on the plastic rotation demand for a lower pier, the plastic rotation demand for a 30m pier with different element number subject to E6 earthquake wave is shown in Fig. 2. From Fig.2 it is can be seen that only one plastic hinge appears at the bottom of the pier with 3 elements, but two or more plastic hinges appear along the pier with the increment of the element number.

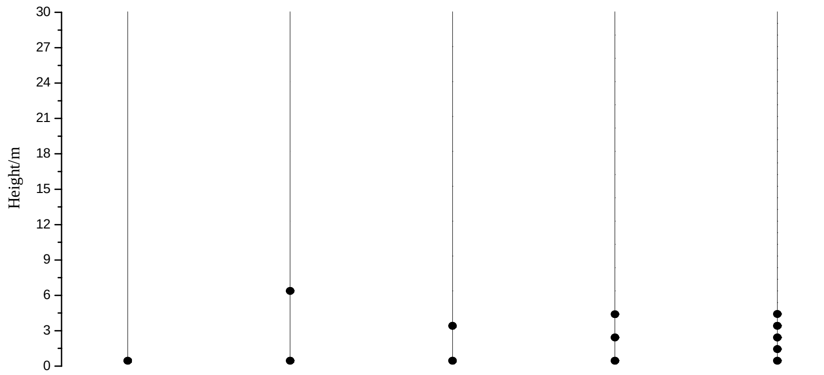

	(a)	(b)	(c)	(d)	(e)
plastic rotation/rad	0.111	0.101	0.065	0.050	0.028
sum of plastic rotation /rad	0.111	0.105	0.111	0.113	0.113

(a) 3 elements (b) 5 elements (c) 10 elements (d) 15 elements (e)30 elements

Fig. 2 Plastic hinges distribution and plastic rotation demand of 30m pier

Fig.2 has shown that with the increase of the element division density, the plastic rotation of the plastic hinge at the bottom of the pier decreased due to multiple plastic hinges appears. In order to getting the rational element division density under different earthquake excitation, the average plastic rotation of various element division densities subjected to 12 earthquakes scaling PGA from 0.2g to 1.2g is shown in Fig. 3.

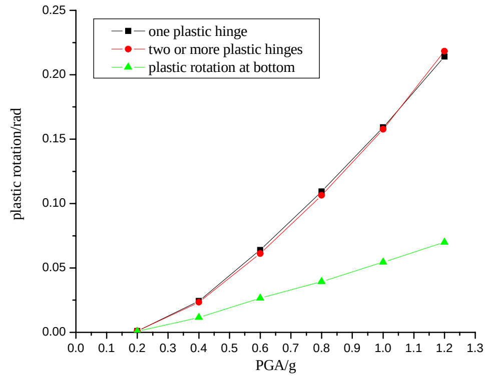

Fig. 3 Plastic rotation demand of different element divisions of 30m pier

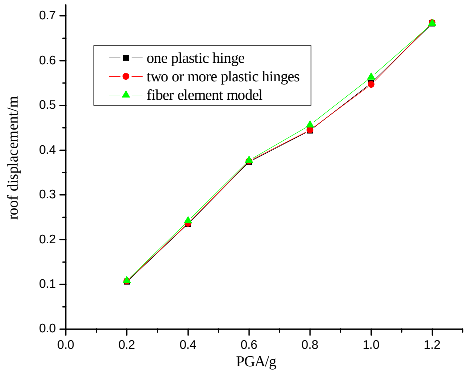

Fig. 4 Top displacement demand of different analytical models of 30m pier

The plastic rotation that the analytical model with 3 elements only has one plastic hinge nearly equals to the plastic rotation sum of the analytical model with 30 elements which has multiple plastic hinges, even to severe earthquake excitation. It proves the accurate plastic rotation demand of low pier can be attained with fewer elements. If the plastic rotation at the pier bottom is considered as plastic rotation of the whole pier that has several plastic hinges, plastic rotation demand of the pier will be underestimated overly. When several plastic hinges emerge in analytical model, the plastic rotation sum of the whole pier, not the plastic rotation at the pier bottom, will be better represent the seismic demand of pier.

Top displacement is an important index that computes the displacement ductility demand, so the rationality of analytical model depends on accuracy of top displacement. The average top displacement of various analytical models subjected to 12 earthquakes scaling PGA from 0.2g to 1.2g is shown in Fig. 4. Top displacements of different analytical models of 30m pier are almost equivalent, even for analytical model with 3 elements.

In order to find out the rule of low pier in emergence of plastic hinges and expansion of plastic zone, the nonlinear dynamic response of 30 elastic-plastic elements model subjected to various PGA, ranging from 0.2g to 1.2g, is evaluated and plotted in Fig 5.

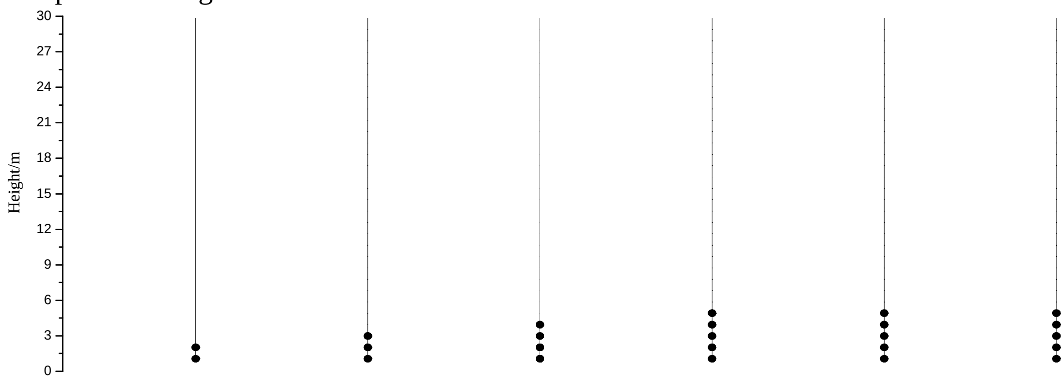

	(a)	(b)	(c)	(d)	(e)	(f)
plastic rotation/rad	0.0007	0.0078	0.0136	0.0185	0.0240	0.0279
plastic rotation sum/rad	0.0010	0.0166	0.0350	0.0576	0.0849	0.1135

(a) PGA=0.2g (b) PGA=0.4g (c) PGA=0.6g (d) PGA=0.8g (e) PGA=1.0g (f) PGA=1.2g

Fig. 5 Plastic hinges formation and plastic zone expansion of 30m pier

From Fig 6，it is proved that in every model all nodal maximum displacements and maximum plastic rotation demands of all plastic hinges occur at same time t=17.61s. The plastic hinge forms and expands at bottom of pier, and plastic rotation demand grows with enhancement of seismic excitation. When mass participation coefficient of first mode is up to 0.87, the seismic response of low pier is dominated by fundamental vibration mode.

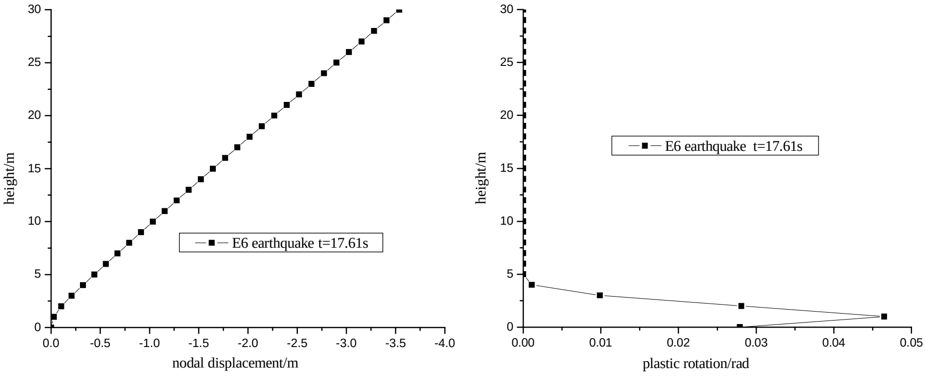

(a) Maximum nodal displacement (b) Maximum plastic rotation

Fig. 6 Maximum nodal displacement and plastic rotation of 30m pier

From above, the accurate plastic rotation and top displacement demand is attained with fewer elements for low pier dominated by fundamental vibration mode.

3.2 Tall pier

Plastic rotation demand of 90m pier subject to E6 earthquake is shown in Fig. 7. Contrast to low pier, two plastic zones at bottom and in middle of the 90m pier emerge under a certain seismic excitation.

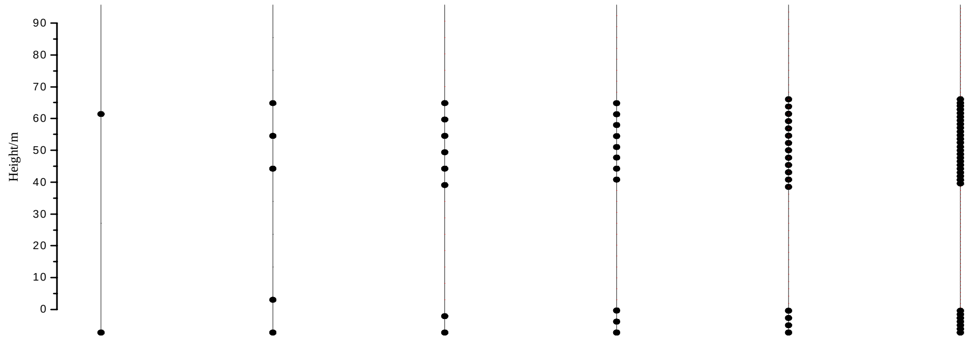

	(a)	(b)	(c)	(d)	(e)	(f)
plastic rotation /rad	0.0429	0.0280	0.0181	0.0141	0.0103	0.0056
plastic rotation sum/rad	0.0577	0.0480	0.0534	0.0534	0.0535	0.0533

(a) 3 elements (b) 10 elements (c) 20 elements (d) 30 elements (e) 45 elements (f) 90 elements

Fig. 7 Plastic hinges distribution and plastic rotation demand of 90m pier

Two or more plastic hinges may emerge for tall pier and element plastic rotation demand is involved in element division density. So it is eligible for tall pier to take element plastic rotation sum as plastic rotation demand. The average plastic rotations of various element division densities subjected to 12 earthquakes scaling PGA from 0.2g to 1.2g are shown in Fig. 8.

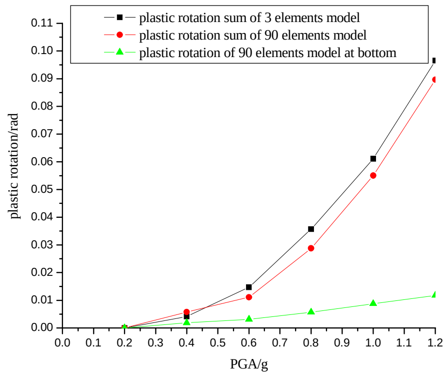

Fig. 8 Plastic rotation demand of different analytical models of 90m pier

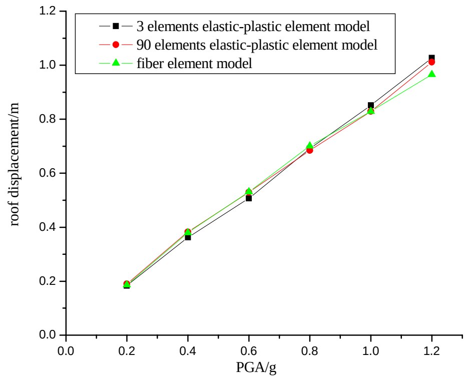

Fig. 9 Roof displacement demand of different analytical models of 90m pier

The plastic rotation sum of 3 elements model slightly differs from the plastic rotation sum of 90 elements model. If the plastic rotation at bottom is considered as plastic rotation of tall pier, plastic rotation demand of the pier will be underestimated overly.
The average top displacement of various analytical models subjected to 12 earthquakes scaling PGA from 0.2g to 1.2g is shown in Fig. 9. Compared to the plastic rotation at bottom, the plastic rotation in the middle is smaller because of closer to the top of the pier. Therefore, the pier top displacements calculated with various element types and various element division densities are closely equivalent. With the enhancement of seismic excitation, plastic rotation in middle of the pier contributes more to top displacement. The difference of elastic-plastic element model and fiber element model will reach 6%~7% subjected to the severe E6 earthquake excitation that peak ground acceleration equals to 1.2g.
Since two or more plastic hinges forms in tall pier, the formation order, magnitude, and location of plastic hinges can reveal effectively the contribution of higher vibration modes to seismic response. The plastic hinge formation and plastic zone expansion of 90m pier subjected to E6 earthquake is shown in Fig. 10.
Compared to second natural period of 90m pier T2=0.55, the higher vibration modes of 90m pier are hardly triggered by the short predominate period, such as E3, E5 and E8 earthquake waves. So 90m pier has similar seismic response to 30m pier. For E1, E4, E6, E7, E9 earthquakes that possess similar predominate period close to second period of pier, the plastic hinges form at bottom of the pier and in the range of 0.4L～0.6L simultaneously. The plastic zone at bottom expands towards topmost, and the plastic one in middle of pier expands towards two ends even more rapidly and wider at same time. Finally, two plastic zones will join and form a larger plastic zone under a severe earthquake excitation. The plastic hinge formation and plastic zone expansion are not sensitive to the predominate periods of earthquakes for 30m pier, but it is quite different for 90m pier. Whether two or more plastic hinge zones appear in 90m pier obviously depend on predominate period of ground motions. When higher natural period of structure approaches predominate period of ground motion, the higher vibration modes are incited and more plastic hinges form.

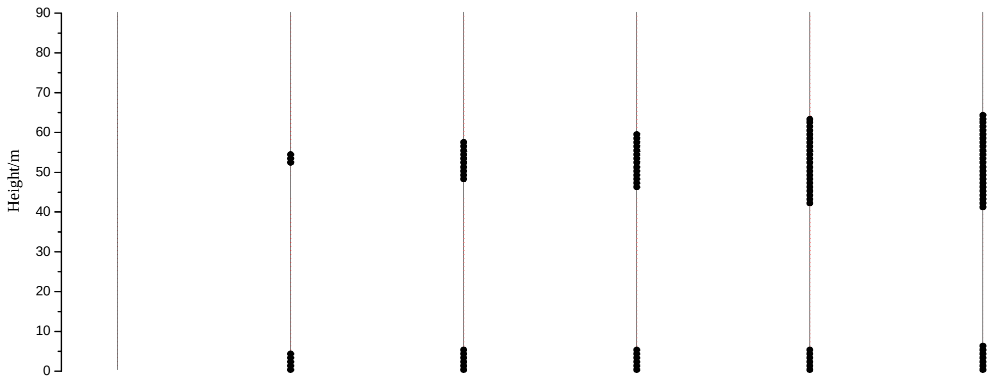

	(a)	(b)	(c)	(d)	(e)	(f)
plastic rotation /rad	0.0000	0.0019	0.0022	0.0034	0.0044	0.0056
plastic rotation sum/rad	0.0000	0.0058	0.0090	0.0199	0.0346	0.0533

(a) PGA=0.2g (b) PGA=0.4g (c) PGA=0.6g (d) PGA=0.8g (e) PGA=1.0g (f)PGA=1.2g

Fig. 10 Plastic hinge formation and plastic zone expansion of 90m pier

From Fig. 11, maximum top displacement occurs at 19.11sec, but plastic rotations at bottom and in the middle of pier don’t reach maximum. The maximum plastic rotation at bottom achieves at 4.87sec, and maximum plastic rotation in the middle of pier achieves at 7.10sec. It is proved that seismic demand of tall pier differs from low pier. Neither maximum displacement nor maximum plastic rotation is up to extremism at the same time.
From above discusses, element plastic rotation demand of tall pier is achieved exactly with elastic-plastic element model using refined model, but accurate top displacement demand depends on application of the fiber element model

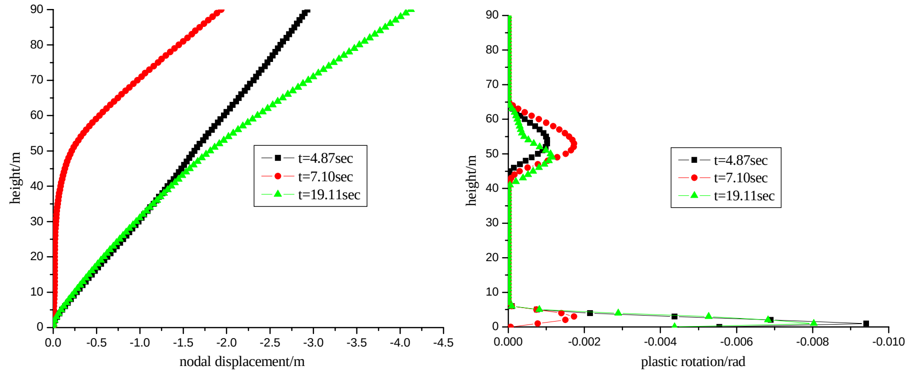

(a) Maximum nodal displacement (b) Maximum plastic rotation

Fig. 11 Maximum nodal displacement and plastic rotation of 90m pier

4. CONCLUSIONS

The nonlinear dynamic history analysis is done for different pier height with different analytical models, and the influence of element division density on structural seismic demand is discussed in the paper. The results show that,

(1) Plastic hinges form in middle of and at bottom of tall pier and plastic zones expand with enhancement of seismic load. Seismic demand of tall pier remarkably differs from low pier when higher vibration modes contribute more.

(2) The seismic parameters have significantly effect on top displacement and plastic rotation demand of tall pier. The higher vibration modes are incited easily when predominate period of earthquake closes to higher natural period of structure. With enhancement of ground motions, the seismic demand of bridge pier increase in manner of expansion of plastic zones and increment of element plastic rotation.

(3) Because higher vibration modes give more contribution to seismic demand of tall pier, its displacement ductility capacity can't achieved through pushover method or formula method. It is necessary to adopt a dynamic method that takes higher vibration modes into account.

(4) The accurate plastic rotation and top displacement demand is attained with fewer elements for low pier. However, accurate top displacement demand of tall pier can't be achieved with elastic-plastic element model even with high-density element division, but can be achieved by fiber element model.

ACKNOWLEDGEMENTS

This research was founded by project number 50578118 by National Natural Science Foundation of China.

REFERENCES

Li Jianzhong, Song Xiaodong, Fan Lichu.(2005). Investigation for displacement ductility capacity of tall piers. *Earthquake engineering and engineering vibration*, **25:1**, 43～48 (in Chinese)

William F. Cofer. (1999). Documentation of Strengths and Weaknesses of Current Computer Analysis Methods for Seismic Performance of reinforced concrete members. Pacific Earthquake Engineering Research Center, University of California, Berkeley

Michael Berry and Marc Eberhard. 2003. Performance models for flexural damage in reinforced concrete columns. Pacific Earthquake Engineering Research Center, University of California, Berkeley,

Taucer, F.F. and Enrico, S. Fiber. 1991. Beam-column model for seismic response analysis of reinforced concrete structures. EERC 91-17

Mohd Hisham. 1994. Nonlinear analysis of prestressed concrete structures under monotonic and cyclic loads. University of California, Berkeley

Mander, J. B.． M. J. N. Priestley and R. Park. 1988. Theoretical stress-strain model for confined concrete. *Journal of The Structural Division, ASCE*, **114:8**, 1804～1826

Silvia Mazzoni, Frank McKenna, Michael H.. 2005. Open System for Earthquake Engineering Simulation User Manual. Pacific Earthquake Engineering Research Center, University of California, Berkeley,
California Department of Transportation. 2001. CALTRANS Seismic Design Criteria, V 1.2. USA
Nie Liying, Li Jianzhong, Fan Lichu. 2004. Elastic-plastic fiber element and element parameter analysis. *Engineering Mechanics*, **21:**3, 15～20 (in Chinese)